

# Bayesian nonparametric sparse VAR models\*

Monica Billio<sup>†§</sup>   Roberto Casarin<sup>†</sup>   Luca Rossini<sup>†‡</sup>

<sup>†</sup> Ca' Foscari University of Venice, Italy   <sup>‡</sup> Free University of Bozen-Bolzano, Italy

**Abstract.** In a high dimensional setting, vector autoregressive (VAR) models require a large number of parameters to be estimated and suffer of inferential problems. We propose a nonparametric Bayesian framework and introduce a new two-stage hierarchical Dirichlet process prior (DPP) for VAR models. This prior allows us to avoid overparametrization and overfitting issues by shrinking the coefficients toward a small number of random locations and induces a random partition of the coefficients, which is the main inference target of nonparametric Bayesian models. We use the posterior random partition to cluster coefficients into groups and to estimate the number of groups.

Our nonparametric Bayesian model with multiple shrinkage prior is well suited for extracting Granger causality networks from time series, since it allows to capture some common features of real-world networks, which are sparsity, blocks or communities structures, heterogeneity and clustering in the strength or intensity of the edges. In order to fully capture the richness of the data, it is therefore crucial that the model used to extract network accounts for weights associated to the edges.

We illustrate the benefits of our approach by extracting network structures from panel data for shock transmission in business cycles and in financial markets. Empirical evidences show that our methodology identifies the most relevant linkages between panel units and clustering effects in the linkages intensity. Also we find that the centrality of the nodes changes across intensity levels.

**Keywords:**

Bayesian nonparametrics; Bayesian model selection; Connectedness; Large vector autoregression; Multilayer networks; Network communities; Shrinkage.

---

\*The authors are grateful to the Guest Editor and the reviewers for their useful comments which significantly improved the quality of the paper. We would like to thank all the conference participants for helpful discussions at: “9th RCEA Bayesian Econometric Workshop” in Rimini; “Internal Seminar” at Ca' Foscari University; “Statistics Seminar” at University of Kent; “9th CFE” in London; “ISBA 2016” in Sardinia; “3rd BAYSM” at University of Florence, “7th ESOBE” in Venice, “10th CFE” in Seville, “7th ICEEE” in Messina, “Bomopav 2017” in Venice, “Big Data in Predictive Dynamic Econometric Modeling” at University of Pennsylvania and “11th BNP” in Paris. We benefited greatly from discussions with Conception Ausin, Francis Diebold, Lorenzo Frattarolo, Pedro Galeano, Jim Griffin, Mark Jensen, Dimitris Korobilis and Stefano Tonellato. This research used the SCSCF multiprocessor cluster system at University Ca' Foscari.

<sup>§</sup>Corresponding author: billio@unive.it (M. Billio). Other contacts: r.casarin@unive.it (R. Casarin) and luca.rossini@unibz.it (L. Rossini).

# 1 Introduction

In the last decade, high dimensional models and large datasets have increased their importance in economics and finance (e.g., see Scott and Varian (2014)). The use of large datasets has been proved to improve the forecasts in large macroeconomic and financial models (e.g., see Carriero et al. (2015), Koop (2013), Stock and Watson (2012)). For analysing and better forecasting them, vector autoregressive (VAR) models have been introduced, which require estimation of a large number of parameters with a few observations. In order to avoid overparametrization, overfitting and dimensionality issues, Bayesian inference and suitable classes of prior distributions have been proposed for VAR (Litterman (1986), Sims (1980, 1992), Doan et al. (1984), Sims and Zha (1998)) and for panel VARs (Canova and Ciccarelli (2004)). See Koop and Korobilis (2010) for a review.

In the literature, it has been proved that these classes of priors may be not effective in dealing with overfitting in very large VAR models. Thus, new priors have been proposed. George et al. (2008) introduce Stochastic Search Variable Selection (SSVS) based on spike-and-slab prior distribution. Wang (2010) combines SSVS prior for the coefficients with graphical prior for the error precision matrix. SSVS has been extended to restricted linear and nonlinear VAR (Korobilis (2013)) and to panel VAR (Koop and Korobilis (2016) and Korobilis (2016)). Ahelgebey et al. (2016a,b) propose Bayesian graphical VAR (BGVAR) and sparse BGVAR to deal with zero restrictions in VAR parameters relying on graphical prior distributions.

We propose a novel Bayesian nonparametric hierarchical prior for VARs, which allows for shrinking the VAR coefficients to multiple random locations and easily extends to other model classes, such as seemingly unrelated regression (SUR) models. The shrinking effects are due to the Lasso-type distribution at the first stage of our hierarchical prior, which improves estimation efficiency, prediction accuracy and interpretation of the temporal dependence structure in time series. We use a Bayesian Lasso prior, which allows us to reformulate the VAR model as a penalized regression problem, in order to determine VAR coefficients to shrink to zero (see Tibshirani (1996) and Park and Casella (2008)). For alternative shrinkage procedures, see also Zou and Hastie (2005) (elastic-net), Zou and Zhang (2009) (Adaptive elastic-net Lasso), Gefang (2014) (Doubly adaptive elastic-net Lasso).

As regards to the second stage of the hierarchy, we use a two-components random mixture distribution on the Normal-Gamma hyperparameters. The first component is a random Dirac point-mass distribution, which induces shrinkage for VAR coefficients; the second component is a Dirichlet process (DP) hyperprior, which induces clustering of the coefficients and allows for inference on the number of clusters.

Our nonparametric Bayesian model with multiple shrinkage prior is well suited for extracting Granger causality networks from time series, since it allows for some common features of real-world networks, that are sparsity (e.g. Ahelgebey et al. (2016b)), communities or blocks (e.g. Casarin et al. (2018)), and heterogeneity in the strength or intensity of the edges (e.g. Bianchi et al. (2018)). In our paper, for the first time, we extract Granger causality networks with clustering effects in the edge intensity. We use the posterior random partition induced by our DP prior to classify the edge intensity (colour) and to estimate the number of colours. The resulting coloured network has a multilayer network representation, with layers given by the different intensity levels. The multilayer representation allows for a better understanding of the network topology and the node centrality.

We contribute to the literature on Bayesian nonparametrics (Ferguson (1973) and Lo (1984)) and its applications to time series (Hirano (2002), Griffin and Steel (2006b), Rodriguez and ter Horst (2008), Taddy and Kottas (2009), Jensen and Maheu (2010), Griffin and Steel (2011), Di Lucca et al. (2013), Bassetti et al. (2014), NietoBarajas and Quintana (2016) and Griffin and Kalli (2018)). See Hjort et al. (2010) for a review.

Up to our knowledge, our paper is the first to provide sparse random measure vector and to apply sparse Bayesian nonparametrics to time series. We substantially improve Hirano (2002), Bassetti et al. (2014) and Griffin and Kalli (2018) by allowing for sparsity in their nonparametric dynamic models. We extend MacLehose and Dunson (2010) by proposing vectors of dependent sparse Dirichlet process priors. As regards to the posterior approximation, we develop a MCMC algorithm building on the slice sampler introduced by Walker (2007), Kalli et al. (2011) and Hatjispyros et al. (2011) for vectors of dependent random measures.

Another contribution of the paper is related to the extraction of networks for shock transmission analysis in business cycle analysis and in financial markets (Diebold and Yilmaz, 2014; Demirer et al., 2018). The network connectedness has a central role in the financial and macroeconomic risk measurement (see Acharya et al. (2012), Billio et al. (2012), Diebold and Yilmaz (2015), Diebold and Yilmaz (2016) and Bianchi et al. (2018)). Our methodology identifies the most relevant linkages and the clustering effects in the linkages intensity.

We find empirical evidence of strength heterogeneity across network edges and centrality heterogeneity of nodes depending on their edge intensity levels. Finally, a comparison of our Bayesian nonparametric model with alternative shrinkage approaches shows the best forecasting performance of our proposed prior.

The paper is organized as follows. Section 2 introduces our sparse Bayesian VAR model. Section 3 presents posterior approximation and network extraction methods. A simulation study illustrates the effectiveness and the efficiency of the

proposed methodology. In Section 4, we present the applications to business cycle and realized volatility datasets. Section 5 concludes.

## 2 A sparse Bayesian VAR model

### 2.1 VAR Models

Let  $N$  be the number of units (e.g. countries, regions or micro studies) in a panel dataset and  $\mathbf{y}_{i,t} = (y_{i,1t}, \dots, y_{i,mt})'$  a vector of  $m$  variables available for the  $i$ -th unit, with  $i = 1, \dots, N$ . A panel VAR is defined as the system of regression equations:

$$\mathbf{y}_{i,t} = \mathbf{b}_i + \sum_{j=1}^N \sum_{l=1}^p B_{ijl} \mathbf{y}_{j,t-l} + \boldsymbol{\varepsilon}_{i,t}, \quad t = 1, \dots, T \text{ and } i = 1, \dots, N, \quad (1)$$

where  $\mathbf{b}_i = (b_{i,1}, \dots, b_{i,m})'$  the vector of constant terms and  $B_{ijl}$  the  $(m \times m)$  matrix of unit- and lag-specific coefficients. We assume that  $\boldsymbol{\varepsilon}_{i,t} = (\varepsilon_{i,1t}, \dots, \varepsilon_{i,mt})'$ , are i.i.d. for  $t = 1, \dots, T$ , with Gaussian distribution  $\mathcal{N}_m(\mathbf{0}, \Sigma_i)$  and that  $\text{Cov}(\boldsymbol{\varepsilon}_{i,t}, \boldsymbol{\varepsilon}_{j,t}) = \Sigma_{ij}$ . Equation 1 can be written in the more compact form as

$$\mathbf{y}_{i,t} = B_i \mathbf{x}_t + \boldsymbol{\varepsilon}_{i,t}, \quad i = 1, \dots, N, \quad (2)$$

where  $B_i = (\mathbf{b}_i, B_{i,11}, \dots, B_{i,1p}, \dots, B_{i,N1}, \dots, B_{i,Np})$  is a  $(m \times (1 + Nmp))$  matrix of coefficients and  $\mathbf{x}_t = (1, \mathbf{x}_{1,t}, \dots, \mathbf{x}_{N,t})'$  is the vector of lagged variables with  $\mathbf{x}_{i,t} = (y_{i,t-1}, \dots, y_{i,t-p})$  for  $i = 1, \dots, N$ .

The system of equations in (2) can be written in the SUR regression form:

$$\mathbf{y}_t = (I_{Nm} \otimes \mathbf{x}_t') \boldsymbol{\beta} + \boldsymbol{\varepsilon}_t \quad (3)$$

where  $\boldsymbol{\beta} = \text{vec}(B)$ ,  $B = (B'_1, \dots, B'_N)$ ,  $\boldsymbol{\varepsilon}'_t = (\boldsymbol{\varepsilon}'_{1t}, \dots, \boldsymbol{\varepsilon}'_{Nt})$ ,  $\otimes$  is the Kronecker product and  $\text{vec}(\cdot)$  the column-wise vectorization operator that stacks the columns of a matrix into a column vector (Magnus and Neudecker, 1999, pp. 31–32).

### 2.2 Prior assumption

The number of parameters in (3) is  $n = Nm(1 + Nmp) + Nm(Nm + 1)/2$ , which can be large for high dimensional panel of time series. In order to avoid overparameterization, unstable predictions and overfitting problem, we follow a hierarchical specification strategy for the prior distributions (e.g., Canova and Ciccarelli (2004), Kaufmann (2010), Bassetti et al. (2014), Billio et al. (2016)). Some classes of hierarchical prior distributions are used to incorporate interdependences

across groups of parameters, with various degrees of information pooling (see Chib and Greenberg (1995) and Min and Zellner (1993)). Other classes of priors (e.g., MacLehose and Dunson (2010), Wang (2010), Bianchi et al. (2018)) are used to induce sparsity. Our new class of hierarchical priors for the VAR coefficients  $\boldsymbol{\beta}$  combines information pooling and sparsity.

We assume that  $\boldsymbol{\beta}$  can be exogenously partitioned in  $M$  blocks,  $\boldsymbol{\beta}_i = (\beta_{i1}, \dots, \beta_{in_i})$ ,  $i = 1, \dots, M$ . In our empirical application, the blocks correspond to the VAR coefficients at different lags. For each block, we introduce shrinking effects by using a Lasso prior  $f_i(\boldsymbol{\beta}_i) = \prod_{j=1}^{n_i} \mathcal{NG}(\beta_{ij}|\mu, \gamma, \tau)$ , where:

$$\mathcal{NG}(\beta|\mu, \gamma, \tau) = \int_0^{+\infty} \mathcal{N}(\beta|\mu, \lambda) \mathcal{Ga}(\lambda|\gamma, \tau/2) d\lambda, \quad (4)$$

is the normal-gamma distribution with  $\mu$ ,  $\gamma$  and  $\tau$ , the location, shape and scale parameter, respectively (see Appendix A). The normal-gamma distribution induces shrinkage toward the prior mean of  $\mu$ . In Bayesian Lasso (Park and Casella (2008)),  $\mu$  is set equal to zero. We extend the Lasso model by allowing for multiple location, shape and scale parameter such that:  $f_i(\boldsymbol{\beta}_i) = \prod_{j=1}^{n_i} \mathcal{NG}(\beta_{ij}|\mu_{ij}^*, \gamma_{ij}^*, \tau_{ij}^*)$ , and reduce curse of dimensionality and overfitting by employing a Dirichlet process (DP) as a prior for the normal-gamma parameters. More specifically, let  $\boldsymbol{\theta}^* = (\mu^*, \gamma^*, \tau^*)$  be the normal-gamma parameter vector, our hierarchical prior for  $\boldsymbol{\theta}^*$  and  $\boldsymbol{\beta}_i$  is

$$\beta_{ij} \stackrel{ind}{\sim} \mathcal{NG}(\beta_{ij}|\boldsymbol{\theta}_{ij}^*), \quad \text{and} \quad \boldsymbol{\theta}_{ij}^* | \mathbb{Q}_i \stackrel{i.i.d.}{\sim} \mathbb{Q}_i, \quad (5)$$

with  $j = 1, \dots, n_i$ , where  $\mathbb{Q}_i$  is a random measure.

Following the strategy in Müller et al. (2004), Pennell and Dunson (2006), Kolossiaty et al. (2013), and Hatjispyros et al. (2011), we assume  $\mathbb{Q}_i$  is a convex combination of a common random measure  $\mathbb{P}_0$  and a block-specific random measure  $\mathbb{P}_i$ , that is

$$\mathbb{Q}_i(d\boldsymbol{\theta}_i) = \pi_i \mathbb{P}_0(d\boldsymbol{\theta}_i) + (1 - \pi_i) \mathbb{P}_i(d\boldsymbol{\theta}_i). \quad (6)$$

The common component  $\mathbb{P}_0$  favours sparsity by shrinking coefficients toward zero, as in standard Bayesian Lasso, i.e.

$$\mathbb{P}_0(d\boldsymbol{\theta}) \sim \delta_{\{(0, \gamma_0, \tau_0)\}}(d(\mu, \gamma, \tau)), \quad \text{with} \quad (\gamma_0, \tau_0) \sim \mathcal{GS}(\gamma_0, \tau_0 | \nu_0, p_0, s_0, n_0), \quad (7)$$

where  $\delta_{\{\boldsymbol{\psi}_0\}}(\boldsymbol{\psi})$  denotes the Dirac measure indicating that the random vector  $\boldsymbol{\psi}$  has a degenerate distribution with mass at the location  $\boldsymbol{\psi}_0$ , and  $\mathcal{GS}(\gamma, \tau | \nu, p, s, n)$  is a Gamma scale-shape distribution with parameters  $\nu$ ,  $p$ ,  $s$  and  $n$  (see Appendix A).

The block-specific component,  $\mathbb{P}_i$ ,  $i > 0$ , is a DP prior (DPP), which shrinks coefficients toward multiple non-zero locations and induces a random partition of

the parameter space and a parameter clustering effect (see, Hirano (2002), Griffin and Steel (2011), Bassetti et al. (2014)), i.e.

$$\mathbb{P}_i(d\boldsymbol{\theta}) \stackrel{i.i.d.}{\sim} \text{DPP}(\tilde{\alpha}, H), \quad \text{with } H \sim \mathcal{N}(\mu|c, d) \cdot \mathcal{GS}(\gamma, \tau|\nu_1, p_1, s_1, n_1) \quad (8)$$

where  $\tilde{\alpha}$  and  $H$  are the DPP concentration parameter and base measure, respectively. See Appendix A for a definition of DPP. For the mixing parameter  $\pi_i$ , we assume a Beta distribution,  $\pi_i \stackrel{i.i.d.}{\sim} \mathcal{Be}(\pi_i|1, \alpha_i)$ .

The amount of shrinkage in  $\mathbb{P}_0$  and  $\mathbb{P}_i$  is determined by the hyperparameters of  $\mathcal{GS}(\nu, p, s, n)$ . In our empirical application, we assume the hyperparameter values  $v_0 = 30$ ,  $s_0 = 1/30$ ,  $p_0 = 0.5$  and  $n_0 = 18$  for the sparse component and  $v_1 = 3$ ,  $s_1 = 1/3$ ,  $p_1 = 0.5$  and  $n_1 = 10$  for the DPP component and  $\alpha_i = 1$  for the mixing parameter, as in MacLehose and Dunson (2010).

For the variance-covariance matrix  $\Sigma$ , we assume a graphical prior distribution as in Carvalho et al. (2007) and Wang (2010), where the zero restrictions on the covariances are induced by a graph  $G$ , that is by an ordered pair of sets  $(N_G, E_G)$ , where  $N_G$  is a vertex set and  $E_G$  a edge set. Conditionally to a specified graph  $G$ , we assume a Hyper Inverse Wishart prior distribution for  $\Sigma$ , that is:

$$\Sigma \sim \mathcal{HIW}_G(b, L), \quad (9)$$

where  $b$  and  $L$  are the degrees of freedom and scale hyperparameters, respectively. See Appendix A for further details on Hyper Inverse Wishart distributions.

The prior over the graph structure is defined as a product of Bernoulli distributions with parameter  $\psi$ , which is the probability of having an edge. That is, a  $m$ -node graph  $G = (N_G, E_G)$ , has a prior probability:

$$p(G) \propto \prod_{i,j} \psi^{e_{ij}} (1 - \psi)^{(1-e_{ij})} = \psi^{|E_G|} (1 - \psi)^{\kappa - |E_G|}, \quad (10)$$

with  $e_{ij} = 1$  if  $(i, j) \in E_G$ , where  $|N_G|$  and  $|E_G|$  are the cardinalities of the vertex and edge sets, respectively,  $\kappa = \binom{|N_G|}{2}$  the maximum number of edges. To induce sparsity we choose  $\psi = 2/(p - 1)$  which would provide a prior mode at  $p$  edges.

In summary, our hierarchical prior in Eq. (5)-(10) is represented through the *Directed Acyclic Graph* (DAG) in Figure 1. Shadow and empty circles indicate the observable and non-observable random variables, respectively. The directed arrows show the causal dependence structure of the model. The left panel shows the priors for  $\boldsymbol{\beta}_i$  and  $\Sigma$ , which are the first stage of the hierarchy. The second stage (right panel) involves the sparse dependent DP prior for the shrinking parameters  $\mu$ ,  $\gamma$  and  $\tau$ .

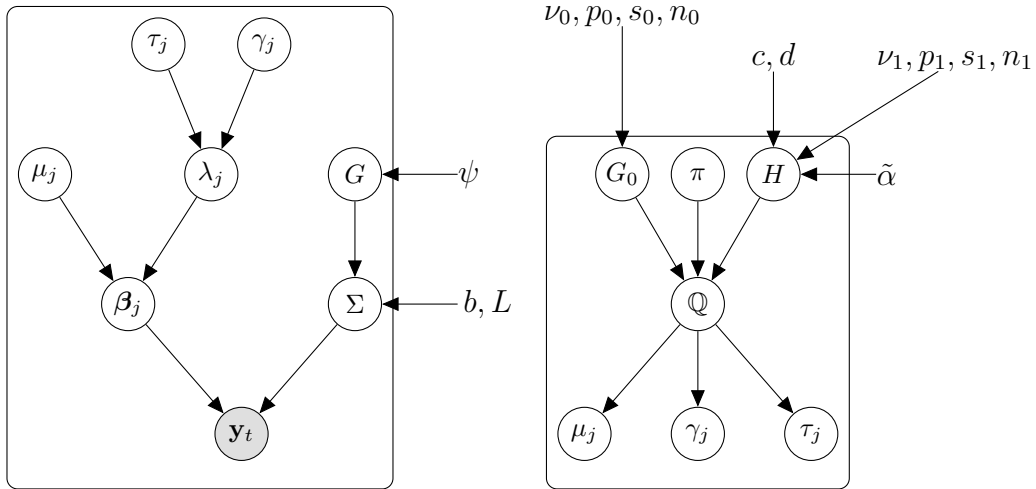


Figure 1: DAG of the Bayesian nonparametric model for inference on VARs. It exhibits the hierarchical structure of priors and hyperparameters. The directed arrows show the causal dependence structure of the model. Left panel is related to the first stage of the hierarchy and right panel to the second stage.

The hierarchical prior in Eq. (5)-(6) has the infinite mixture representation with a countably infinite number of clusters, which is one of the appealing feature of Bayesian nonparametrics:

$$f_i(\beta_i | Q_i) = \sum_{k=0}^{\infty} \check{w}_{ik} \mathcal{NG}(\beta_i | \check{\theta}_{ik}), \quad (11)$$

where

$$\check{w}_{ik} = \begin{cases} \pi_i, & k = 0, \\ (1 - \pi_i)w_{ik}, & k > 0, \end{cases} \quad \check{\theta}_{ik} = \begin{cases} (0, \gamma_0, \tau_0), & k = 0, \\ (\mu_{ik}, \gamma_{ik}, \tau_{ik}), & k > 0. \end{cases}$$

See Appendix B for a proof. This representation shows that our prior not only shrinks coefficients to zero as in Bayesian Lasso (Park and Casella (2008)) or Elastic-net (Zou and Hastie (2005)), but also induces a probabilistic clustering effect in the parameter set as in other Bayesian nonparametric models (Hirano (2002) and Bassetti et al. (2014)).

Our prior places no bounds on the number of mixture components and can fit arbitrary complex distribution. Nevertheless, since the mixture weights,  $w_{ik}$ 's, decrease exponentially quickly only a small number of clusters will be used to model the data a priori. As shown in Antoniak (1974), the prior number of clusters is a

random variable with distribution driven by the concentration parameter  $\tilde{\alpha}$ . The attractive property of this model is that the number of mixture components can be inferred from the data without being specified in advance (Teh, 2011) as it happens in finite mixture modelling. A similar approach for finite mixture models would be model averaging or model selection for the number of components, but it can be nontrivial to design efficient MCMC samplers (e.g. Richardson and Green (1997)). Meanwhile, for Bayesian nonparametrics, there are relatively simple and flexible samplers for posterior approximation (e.g. Kalli et al. (2011)).

Finally, our framework is quite general and flexible and it can be applied to different parameter partitioning. For example, in a panel VAR model the blocks of parameters can be chosen to be the coefficients of the unit-specific equation. Moreover, it can be extended by introducing lag-specific shrinking effects as in a Minnesota type prior and dependent clustering features as in beta-dependent Pitman-Yor prior (Bassetti et al., 2014; Taddy, 2010; Griffin and Steel, 2011). We leave these issues for future research.

## 3 Posterior inference

### 3.1 Sampling method

Since the posterior distribution is not tractable, Bayesian estimator cannot be obtained analytically. In this paper we rely on simulation based inference methods, and develop a Gibbs sampler algorithm for approximating the posterior distribution. For the sake of simplicity and without loss of generality we shall describe the sampling strategy for the two-block case, i.e.  $M = 2$ .

In order to develop a more efficient MCMC procedure, we follow a data augmentation approach. For each block  $i = 1, 2$  we introduce two sets of allocation variables,  $\xi_{ij}, d_{ij}, j = 1, \dots, n_i$ , a set of stick-breaking variables,  $v_{ij}, j = 1, 2, \dots$  and a set of slice variables,  $u_{ij}, j = 1, \dots, n_i$ . The allocation variable,  $\xi_{ij}$ , selects the sparse component  $\mathbb{P}_0$ , when  $\xi_{ij}$  is equal to zero and the non-sparse component  $\mathbb{P}_i$ , when it is equal to one. The second allocation variable,  $d_{ij}$ , selects the component of the Dirichlet mixture  $\mathbb{P}_i$  to which each single coefficient  $\beta_{ij}$  is allocated to. The sequence of stick-breaking variables define the mixture weights, whereas the slice variable,  $u_{ij}$ , allow us to deal with the infinite number of mixture components by identifying a finite number of stick-breaking variables to be sampled and an upper bound for the allocation variables  $d_{ij}$ .

We demarginalize the Normal-Gamma distribution by introducing a latent



variable  $\lambda_{ij}$  for each  $\beta_{ij}$  and obtain the joint posterior distribution

$$\begin{aligned}
f(\Theta, \Sigma, \Lambda, U, D, V, \Xi|Y) &\propto \prod_{t=1}^T (2\pi|\Sigma|)^{-1/2} \exp\left(-\frac{1}{2}(y_t - X_t'\beta)'\Sigma^{-1}(y_t - X_t'\beta)\right) \\
&\prod_{j=1}^{n_1} f_1(\beta_{1j}, \lambda_{1j}, u_{1j}, d_{1j}, \xi_{1j}) \prod_{j=1}^{n_2} f_2(\beta_{2j}, \lambda_{2j}, u_{2j}, d_{2j}, \xi_{2j}) \cdot \\
&\prod_{k>1} \mathcal{Be}(v_{1k}|1, \alpha)\mathcal{Be}(v_{2k}|1, \alpha)\mathcal{HILW}_G(b, L)\mathcal{GS}(\gamma_0, \tau_0|\nu_0, p_0, s_0, n_0) \cdot \\
&\prod_{k>1} \mathcal{N}(\mu_{1k}|c, d)\mathcal{GS}(\gamma_{1k}, \tau_{1k}|\nu_1, p_1, s_1, n_1)\mathcal{N}(\mu_{2k}|c, d)\mathcal{GS}(\gamma_{2k}, \tau_{2k}|\nu_1, p_1, s_1, n_1).
\end{aligned} \tag{12}$$

where  $U = \{u_{ij} : j = 1, 2, \dots, n_i \text{ and } i = 1, 2\}$  and  $V = \{v_{ij} : j = 1, 2, \dots \text{ and } i = 1, 2\}$  are the collections of slice variables and stick-breaking components, respectively;  $D = \{d_{ij} : j = 1, 2, \dots, n_i \text{ and } i = 1, 2\}$  and  $\Xi = \{\xi_{ij} : j = 1, 2, \dots, n_i \text{ and } i = 1, 2\}$  are the allocation variables;  $\Theta = \{(\mu_0, \gamma_0, \tau_0), (\mu_{ik}, \gamma_{ik}, \tau_{ik}) : i = 1, 2 \text{ and } k = 1, 2, \dots\}$  are the atoms;  $\pi = (\pi_1, \pi_2)$  are the block-specific probabilities of shrinking coefficients to zero and

$$\begin{aligned}
f_i(\beta_{ij}, \lambda_{ij}, u_{ij}, d_{ij}, \xi_{ij}) &= (\mathbb{I}(u_{ij} < \tilde{w}_{d_{ij}})\mathcal{N}(\beta_{ij}|0, \lambda_{ij})\mathcal{Ga}(\lambda_{ij}|\gamma_0, \tau_0/2))^{1-\xi_{ij}} \cdot \\
&(\mathbb{I}(u_{ij} < w_{id_{ij}})\mathcal{N}(\beta_{ij}|\mu_{id_{ij}}, \lambda_{ij})\mathcal{Ga}(\lambda_{ij}|\gamma_{id_{ij}}, \tau_{id_{ij}}/2))^{\xi_{ij}} \pi_i^{1-\xi_{ij}} (1 - \pi_i)^{\xi_{ij}}.
\end{aligned} \tag{13}$$

See Appendix (B) for a derivation.

We obtain random samples from the posterior distributions by Gibbs sampling. The Gibbs sampler iterates over the following steps using the conditional independence between variables as described in Appendix C:

1. The slice and stick-breaking variables  $U$  and  $V$  are updated given  $[\Theta, \beta, \Sigma, G, \Lambda, D, \Xi, \pi, Y]$ ;
2. The latent scale variables  $\Lambda$  are updated given  $[\Theta, \beta, \Sigma, G, U, V, D, \Xi, \pi, Y]$ ;
3. The parameters of the Normal-Gamma distribution  $\Theta$  are updated given  $[\beta, \Sigma, G, \Lambda, U, V, D, \Xi, \pi, Y]$ ;
4. The coefficients  $\beta$  of the VAR model are updated given  $[\Theta, \Sigma, G, \Lambda, U, V, D, \Xi, \pi, Y]$ ;
5. The matrix of variance-covariance  $\Sigma$  is updated given  $[\Theta, \beta, G, \Lambda, U, V, D, \Xi, \pi, Y]$ ;

6. The graph  $G$  is updated given  $[\Theta, \boldsymbol{\beta}, \Sigma, \Lambda, U, V, D, \Xi, \pi, Y]$ ;
7. The allocation variables  $D$  and  $\Xi$  are updated given  $[\Theta, \boldsymbol{\beta}, \Sigma, G, \Lambda, U, V, \pi, Y]$ ;
8. The probability,  $\pi$ , of shrinking-to-zero the coefficient is updated given  $[\Theta, \boldsymbol{\beta}, \Sigma, G, \Lambda, U, V, D, \Xi, Y]$ .

### 3.2 Network extraction

Pairwise Granger causality has been used to extract linkages and networks describing relationships between variables of interest, e.g. financial and macroeconomic linkages (Billio et al., 2012; Barigozzi and Brownlees, 2016). The pairwise Granger causality approach does not consider conditioning on relevant covariates thus generating spurious causality effects. The conditional Granger approach includes relevant covariates, however the large number of variables relative to the number of data points can lead to overparametrization and consequently a loss of degree of freedom and inefficiency in correctly gauging the causal relationships (see (Ahelgebey et al., 2016a,b)). Our hierarchical prior combining Bayesian Lasso and Dirichlet process prior allows us to extract the network while reducing overfitting and curse of dimensionality problems. Also, it allows to capture various stylized facts recently investigated in financial networks, such as the presence of blocks or communities structures (e.g., Casarin et al. (2018)), and the relevance of the edge weights in the analysis of network topology and nodes centrality (e.g., Bianchi et al. (2018)).

We denote with  $G_l = (V_l, E_l)$  the graph at lag  $l$ , where  $V_l = \{1, \dots, N\}$  is the vertex set and  $i \in V_l$  the node associated with the variable  $y_{it}$ . We assume that there exists an edge  $\{i, j\} \in E_l$  between  $i, j \in V_l$  if  $B_{ij,l} \neq 0$ . The adjacency matrix  $A_l$  associated with  $G_l$  has  $(i, j)$ -th element

$$a_{ij,l} = \begin{cases} 1, & \text{if } \xi_{\varphi(i,j),l} = 0, \\ 0, & \text{otherwise,} \end{cases}$$

where  $\varphi(i, j) = N(i-1) + j$  and  $\xi_{k,l}$  is the maximum a posteriori (MAP) estimate of the shrinking-to-zero indicator variable for the parameter  $\beta_{k,l}$ . The Dirichlet process prior allows us to assign the weights to the edges and to cluster them into groups. To this aim, we apply the least square clustering proposed originally in Dahl (2006). The method is based on the posterior pairwise probabilities of joint classification  $P(d_{il} = d_{jl} | Y, \xi_{i,l} = 1, \xi_{j,l} = 1)$  approximated as

$$p_{ij,l} = \frac{1}{H} \sum_{h=1}^H \delta_{d_{i,l}^h}(d_{j,l}^h), \quad (14)$$

where we use the allocation variable MCMC draws  $d_{i,l}^h$ , with  $h = 1, \dots, H$  and  $i = 1, \dots, \tilde{m}$ , where  $H$  is the number of MCMC iterations and  $\tilde{m}$  is the number of nonzero coefficient. We can detect the presence of different clusters from the co-clustering matrix based on the location atom,  $\mu_{kl}^{*,h}$ , generated at each iteration of the MCMC sampler and build up from the least square marginal clustering. The least square marginal clustering is the clustering  $\tilde{D}_l$ , which minimizes the sum of squared deviations from the pairwise posterior probability

$$\tilde{D}_l = \arg \min_{D \in \{D^1, \dots, D^H\}} \sum_{i=1}^{\tilde{m}} \sum_{j=1}^{\tilde{m}} \left( \delta_{d_{i,l}^h}^h(d_{j,l}^h) - p_{ij,l} \right)^2. \quad (15)$$

Equation (15) allows us to estimate a finite number  $\tilde{K}$  of edge intensity levels (colours) and to define the weighted graph  $G_l = (V_l, E_l, C_l)$ , where  $C_l$  is the edge weights matrix with elements

$$c_{ij,l} = \begin{cases} \tilde{\mu}_{1l}^* & \text{if } \tilde{d}_{\varphi(i,j),l} = 1 \text{ and } \xi_{\varphi(i,j),l} = 0 \\ \tilde{\mu}_{2l}^* & \text{if } \tilde{d}_{\varphi(i,j),l} = 2 \text{ and } \xi_{\varphi(i,j),l} = 0 \\ \vdots & \vdots \\ \tilde{\mu}_{\tilde{K}l}^* & \text{if } \tilde{d}_{\varphi(i,j),l} = \tilde{K} \text{ and } \xi_{\varphi(i,j),l} = 0 \\ 0 & \text{if } \xi_{\varphi(i,j),l} = 1 \end{cases} \quad (16)$$

$i, j = 1, \dots, m$ , indicating the strengthness of relationship between nodes, that is the magnitude of the linkages between economic variables.

A better understanding of the connectivity patterns can be achieved using the edge weights matrix and the multilayer network representation of the coloured graph. Note that the multilayer representation is possible thanks to the posterior partition of the edges in a finite number of groups. The topology of the network can be analyzed at the level of the single layer and the vertex out-degree,  $\omega_{il}^+$ , of the node  $i$  at lag  $l$  can be decomposed in  $\tilde{K}$  different strengthness levels

$$\omega_{il}^+ = \sum_{j=1}^m a_{ij,l} = \sum_{k=1}^{\tilde{K}} \omega_{il,k}^+, \quad \text{where } \omega_{il,k}^+ = \sum_{j=1}^m a_{ij,l} \mathbb{I}(c_{ij,l} = \tilde{\mu}_{kl}^*).$$

Similarly, it is possible to decompose the vertex in-degree,  $\omega_{il}^-$ .

### 3.3 Simulation experiments

We study the goodness of fit of our nonparametric model presented in Section 2 and, following the standard practice in Bayesian nonparametric analysis (see, e.g. Griffin

and Steel (2006a), Griffin and Steel (2011), Griffin and Kalli (2018)), we simulate data from a parametric model which is in the family of the likelihood of our model. We consider a VAR(1) model

$$\mathbf{y}_t = B\mathbf{y}_{t-1} + \boldsymbol{\varepsilon}_t, \quad \boldsymbol{\varepsilon}_t \stackrel{i.i.d.}{\sim} \mathcal{N}_m(\mathbf{0}, \Sigma) \quad t = 1, \dots, 100,$$

where the dimension of  $\mathbf{y}_t$  is alternatively  $m = 20$  (small),  $m = 40$  (medium) and  $m = 80$  (large). We consider two settings for the coefficient matrix  $B$ . In the first one, we consider a block-diagonal matrix  $B$  with  $(4 \times 4)$  blocks  $B_j$  ( $j = 1, \dots, m/4$ ) on the main diagonal and i.i.d. elements  $b_{lk,j} \sim \mathcal{U}(-1.4, 1.4)$ ,  $l, k = 1, \dots, 4$  checked for the weak stationarity condition of the VAR. The block-diagonal structure which mimicks the block structures detected in many real word networks, and recently investigated by Casarin et al. (2018) for financial networks. In the second setting, we follow Korobilis (2016) and set the coefficients either to zero, or to uniform random values. More specifically we consider a random matrix  $B$  of dimension  $(80 \times 80)$ , select randomly 150 elements and draw their values from the uniform  $\mathcal{U}(-1.4, 1.4)$ . The remaining 6250 elements are set to zero. The matrix generated is then checked for weak stationarity.

In all the experiments, we have chosen the hyperparameters for the sparse and non-sparse components as in Section 2.2 and the hyperparameters of the Hyper-Inverse Wishart as in Section 2.2, where the degree of freedom parameter is  $b_0 = 3$  and the scale matrix is  $L = I_n$ . For all settings, we iterated 5,000 times the Gibbs sampler described in Section 3 and discarded the first 500 samples following a graphical dissection of the posterior progressive averages. The remaining samples have been used to approximate the posterior distribution.

We analyse the efficiency of the MCMC samples by employing standard convergence diagnostic measures. Since in a data augmentation framework, the mixing of the MCMC may depend on the autocorrelation in both parameter and latent variable samples, we focus on  $\lambda_{ij}$ ,  $u_{ij}$  and  $\beta_{ij}$ . The convergence diagnostic for  $\lambda_{ij}$ , after removing 500 burn-in iterations, indicates the chain has converged (see Table 1). The inefficiency factor and the autocorrelation at lag 10 on the original sample suggest high levels of dependence in the sample, which can be mitigated by thinning the chains. We keep only every 5th sample and obtain substantial reduction of sample autocorrelation. See Supplementary Material for further details.

We use the thinned MCMC samples of  $\Xi$  to estimate the network adjacency matrix and the samples of  $D$  to estimate the number of colours and classify the edge intensity. We provide in Figure 2 the resulting causality network. In each coloured graph the nodes represent the  $n$  variables of the VAR model, and a clockwise-oriented edge between two nodes  $i$  and  $j$  represents a non-null coefficient for the variable  $y_{j,t-1}$  in the  $i$ -th equation of the VAR. The blue edges represent negative

	CD	KS	INEFF		Acf(10)	
			before	after	before	after
$m = 20$	-0.629	0.3667	13.5092	7.0346	0.1724	0.0188
$m = 40$	-1.197	0.002	21.3259	8.5001	0.3366	0.1334
$m = 80$ block	-1.354	0.5806	20.1303	9.6897	0.3147	0.1229
$m = 80$ random	2.451	0.0158	17.6933	5.8095	0.267	0.0185

Table 1: Geweke (CD) and Kolmogorov-Smirnov (KS) convergence test; inefficiency factor (INEFF) and autocorrelation (Acf) computed at lag 10 for the  $\mathcal{L}^2$  norm of  $\lambda_{ij}$  for each experiments on the whole (before) and thinned (after) MCMC samples.

coefficients, while the red ones represent positive coefficients. See Supplementary Material for further results.

We compare our prior (BNP) with the Bayesian Lasso (B-Lasso, Park and Casella (2008)), the Elastic-net (EN, Zou and Hastie (2005)) and Stochastic Search Variable Selection (SSVS) of George et al. (2008). For the SSVS, we assume the default hyperparameters values  $\tau_1^2 = 0.0001$ ,  $\tau_2^2 = 4$  and  $\pi = 0.5$ . Following Korobilis (2016), we use the mean square deviation (MSD) for measuring the performance of the four different priors. For each parameter setting we generate 50 independent datasets and apply the models under comparison. The boxplots in Figure 2 show the MSD statistics for the 50 experiments. Increasing the dimensionality from 20 (left panel) to 80 (right panel) leads to an improvement of the performance of our prior. The results confirm the best performance of our prior in large dimension settings. The comparison in the other settings (see Supplementary Material) confirms the result.

## 4 Empirical Applications

### 4.1 Measuring business shock transmission

Following the literature on international business cycles (Kose et al., 2003, 2010; Francis et al., 2017; Kaufmann and Schumacher, 2017) we consider a multi-country macroeconomic dataset to investigate the business shock transmission effects across different countries. We apply the proposed Bayesian nonparametric model to the dataset and, following Diebold and Yilmaz (2015), extract a network of macroeconomic linkages. Our model allows us: (i) to study the shock transmission mechanism at different lags; (ii) to identify the most relevant linkages between countries; (iii) to cluster the linkages into different levels of intensity.

We consider the quarterly GDP growth rate (logarithmic first differences) for

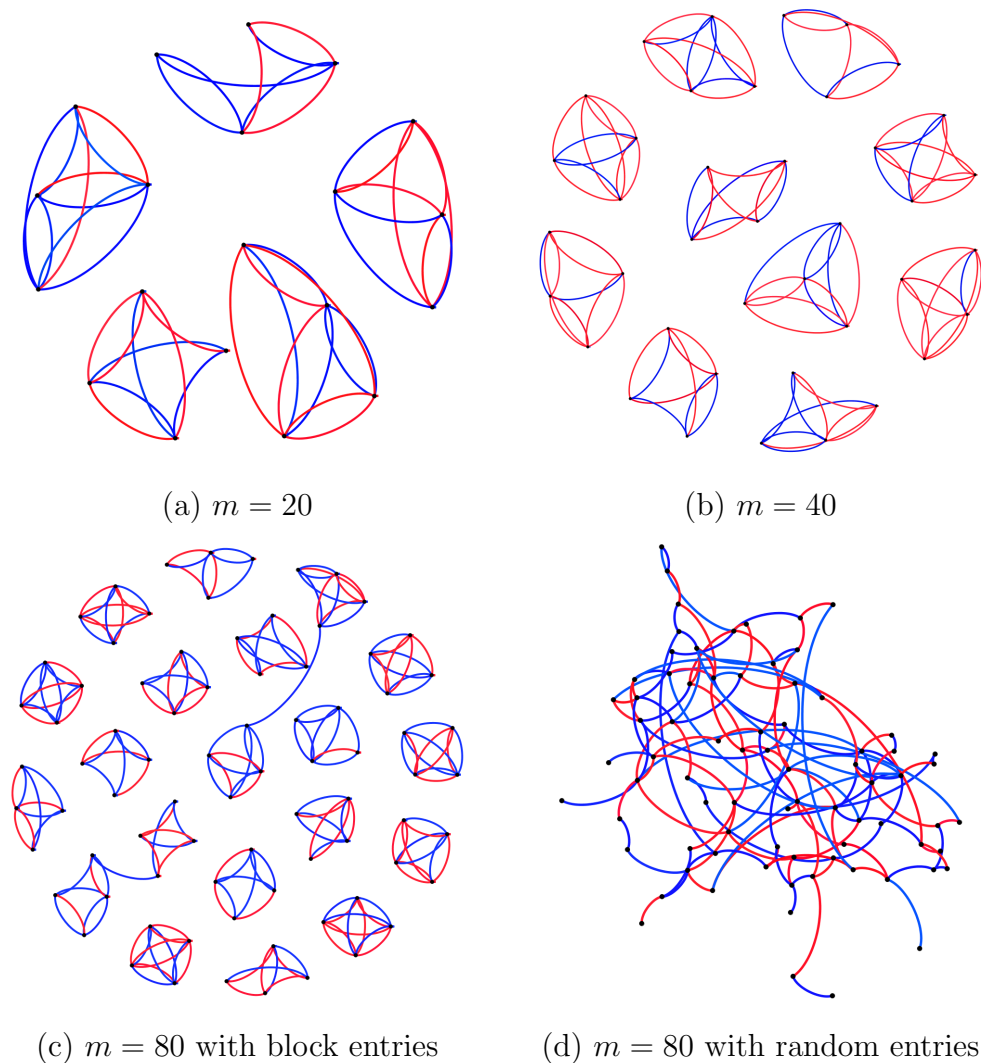


Figure 2: Weighted network for different model dimensions  $m = 20$  (panel (a)),  $m = 40$  (panel (b)) and  $m = 80$ , with block entries (panel (c)) and with random entries (panel (d)). Blue edges mean negative weights and red ones represent positive weights, while the edges are clockwise-oriented.

OECD countries from the first quarter of 1961 to the second quarter of 2015, for a total of  $T = 215$  observations. Due to missing values in some of the GDP series, we choose a subset of high industrialised OECD countries and focus on two big macroareas:

- Rest of the World: Australia, Canada, Japan, Mexico, South Africa, Turkey,

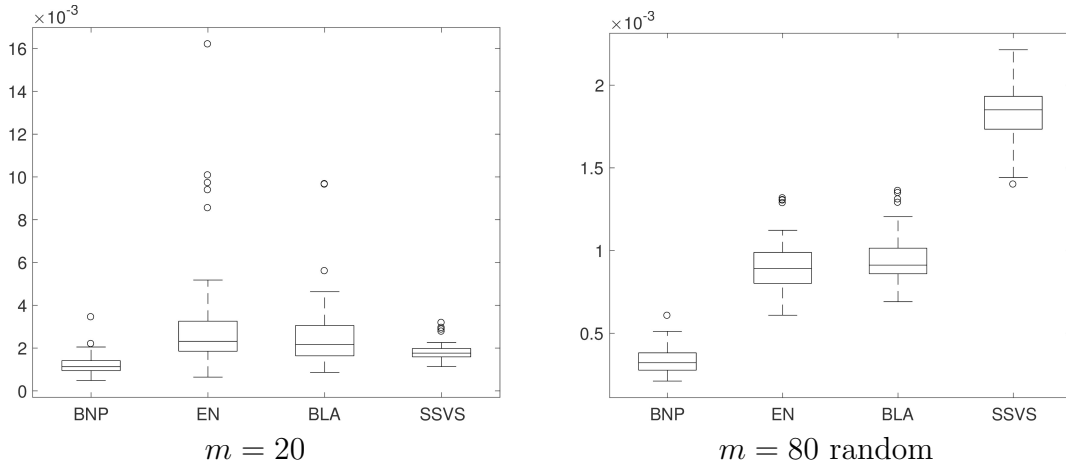


Table 2: Boxplot of MSD statistics in the Monte Carlo exercise when  $m = 20$  (left panel) and when  $m = 80$  with random entries (right panel) for our Bayesian nonparametric model (BNP), Elastic-net (EN), Bayesian Lasso (BLA) and Stochastic Search Variable Selection (SSVS).

United States;

- Europe: Austria, Belgium, Denmark, Finland, France, Germany, Greece, Ireland, Iceland, Italy, Luxembourg, Netherlands, Norway, Portugal, Spain, Sweden, Switzerland, United Kingdom;

We apply a VAR(4) with the prior setting of Section 2 and run the Gibbs sampling described in Section 3. The posterior probability of a macroeconomic linkage is 0.13, which provides evidence of sparsity in the network and indicates that a small proportion of linkages is responsible for shocks transmission between countries. The posterior number of clusters and the co-clustering matrix (see Supplementary Material) reveals the existence of three levels of linkage intensity, customarily called “negative”, “positive” and “strong positive”. Figure 3 draws the weighted (or coloured) networks at different time lags. The blue edges represent negative weights, while the red ones represent positive weights. In each coloured graph, the nodes represent the  $m$  variables of the VAR model, and a clockwise-oriented edge from node  $j$  to node  $i$  represents a non-null coefficient for the variable  $y_{j,t-1}$  in the  $i$ -th equation of the VAR. In a multi-layer graph representation, each intensity level (or edge colour) identifies the set of nodes and edges belonging to a specific layer. The network connectivity and nodes centrality can be investigated either at the global level, or for each single layer.

The dynamical structure of the directional connectedness received from other

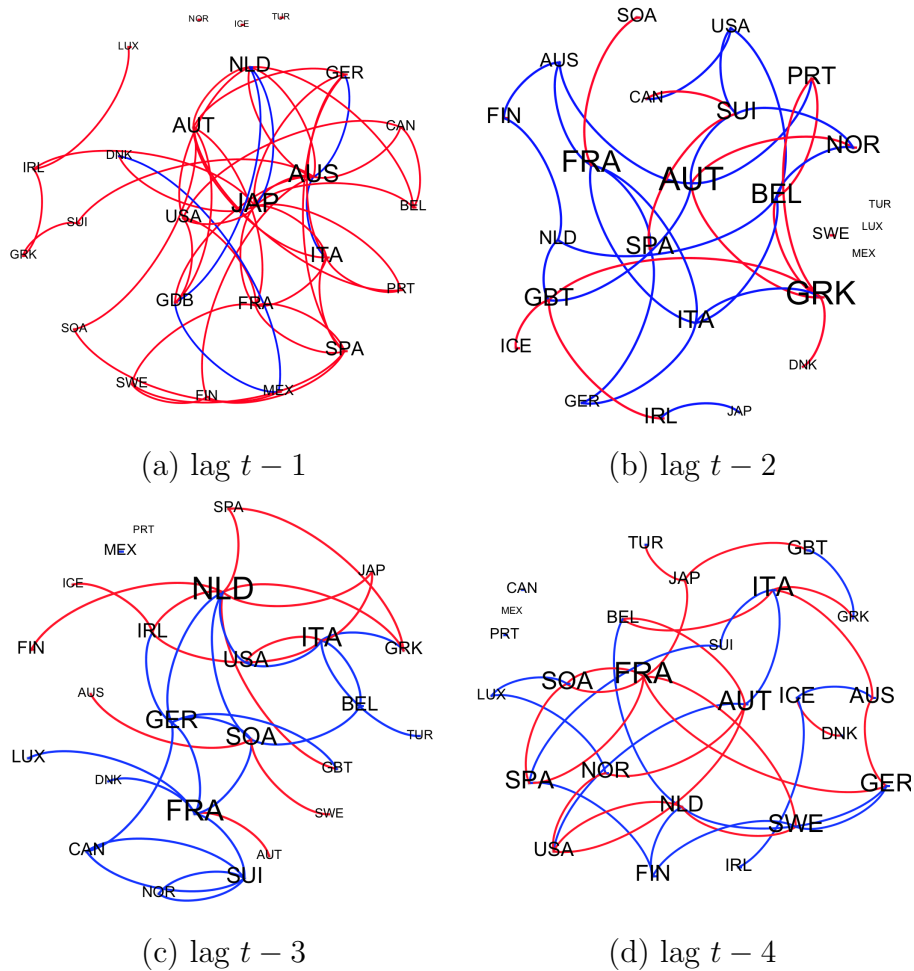


Figure 3: Weighted shock transmission networks of GDP for OECD countries at lag: (a)  $t - 1$ , (b)  $t - 2$ , (c)  $t - 3$ , (d)  $t - 4$ , where blue edges represent negative weights and red ones positive weights. Nodes' size is based on the node degree and the edges are clockwise-oriented.

countries (in-degree) or transmitted to other countries (out-degree) shows that:

- at lags  $t - 1$  and  $t - 2$ , core European countries (Austria, Belgium, Finland, France, Germany, Netherlands) are mainly receivers, whereas the periphery European countries (Greece, Ireland, Italy, Portugal, Spain) transmit the highest percentage of shocks. In the other lags, core countries receive and transmit a high percentage of shocks;
- at lag  $t - 1$ , Japan is the country with the highest out-degree, meaning that



it is transmitting the highest percentage of shocks to other countries, followed by Spain and Austria;

- at lag  $t - 1$ , Australia is the country with the highest in-degree, meaning that it receives the highest percentage of shocks from other countries, followed by France, Germany and United Kingdom;
- at higher lags, Greece, France, Austria, Germany, Italy and Netherlands are central countries in the business shock transmission.

We analyse the network topology (see Table 3) and find that the density of the graph and the average degree at the first lag are larger than at other lags, which means that there is a decay over lags in the shock transmission effects. The average graph-distance between all pair of nodes (average path length) decreases over lags, which suggests that the diameter of the largest connected component and the network complexity are reducing.

When edge intensity levels are considered (coloured edges in Figure 3), we find that, at lag  $(t - 1)$ , 88% of the linkages represent either positive and strong positive effects and that most of them are between European countries. At other lags, negative effects between rest of the world countries are shown. European countries have positive linkage strength between them, and a negative one with the rest of the world. These results are confirmed by the network connectivity analysis in Table 3. Network average degree at the first lag (2.92) is mainly driven by positive and strong positive edge intensities (2.64). At the second lag, the red and blue coloured network have similar average degree, whereas at the third and fourth lag, negative linkages prevail over positives. The density for the different networks behaves similarly.

Analysing the positive linkages subgraph (red graph) and the negative linkages subgraph (blue graph) we find that nodes can play different role in the network connectivity. At the first lag, the central country, i.e. Japan, remains central in the red graph, but is less central than Netherlands in the blue graph. At lag  $(t - 2)$ , Greece is central in the red graph and Italy in the blue one, and both countries are less central than Austria in the overall network. Similar heterogeneity in the node centrality can be found in the remaining lags.

The proposed Bayesian nonparametric model (BNP-Lasso) allows not only for a better understanding of the connectivity patterns in business cycles but also for a better forecasting, when compared to other model priors, such as Elastic-Net (EN), Bayesian Lasso (B-Lasso) and SSVS.

Our forecasting results are based on one-step-ahead forecasting process with a rolling window of 38 years (152 quarterly observations), and a forecast evaluation period of 14 years ranging from the first quarter of 2001 to the second quarter of

	Links	Avg Degree	Density	Avg Path Length
$t - 1$	73	2.92	0.122	3.423
$t - 1$ blue	7	0.28	0.012	1.143
$t - 1$ red	66	2.64	0.11	2.587
$t - 2$	45	1.80	0.075	3.211
$t - 2$ blue	22	0.88	0.037	2.634
$t - 2$ red	23	0.92	0.038	2.033
$t - 3$	41	1.64	0.069	2.479
$t - 3$ blue	25	1.00	0.042	2.268
$t - 3$ red	16	0.64	0.027	1.667
$t - 4$	52	2.08	0.086	2.718
$t - 4$ blue	32	1.28	0.053	1.435
$t - 4$ red	20	0.80	0.033	1.791

Table 3: The network statistics for single layers networks divided by positive (red) and negative (blue) edge intensity. The average path length represents the average graph-distance between all pairs of nodes. Connected nodes have graph distance 1.

2015 (58 observations). We assess the goodness of our forecasts using the root mean square errors (RMSEs) and average log predictive score. The log predictive score is commonly viewed as the broadest measure of density accuracy, see Geweke and Amisano (2010).

In Table 4, we report the metrics average value for the BNP-Lasso in the Rest-of-the-World and European countries. For the other models, we report the ratios of each model’s RMSE to the benchmark model, such that entries less than 1 indicate that the given model yields forecasts more accurate than those from the baseline; differences in score relative to the benchmark, such that a positive number indicates a model beats the baseline. In Supplementary Material, we report the results for each country. Following RMSEs and log predictive scores in Table 4, the point and density forecast of the benchmark model are the most accurate for both Rest of the World and European countries. The out-of-sample results are thus consistent with in-sample results obtained in the simulation experiments.

## 4.2 Risk Connectedness in European Financial Markets

Based on the literature on risk connectedness among financial institutions and markets (see Hautsch et al. (2015) and Diebold and Yilmaz (2014)), we construct daily realized volatilities using intraday high-low-close price indexes of 118 institutions of the Euro Stoxx 600 obtained from Datastream, from January 3, 2005 to September 19, 2014. The dataset consists of 42 Banks, 31 Financial services, 31

	Rest of the World		Europe	
	RMSE	log predictive	RMSE	log predictive
BNP-Lasso	0.4083	-0.5525	0.4781	-0.7163
EN	1.0407	-0.0604	1.0029	-0.1107
B-Lasso	1.0308	-0.0747	0.9960	-0.1529
SSVS	1.1458	-0.1332	1.0895	-0.1333

Table 4: RMSE and log predictive score for our Bayesian nonparametric sparse model (BNP-Lasso), and RMSE ratios and score differences for all other models, Elastic-Net (EN), Bayesian Lasso (B-Lasso) and SSVS for the mean over the Rest of the World and European countries.

Insurance companies and 22 Real estates and covers the main European countries: Austria, Belgium, Finland, France, Germany, Greece, Ireland, Italy, Luxembourg, Netherlands, Portugal and Spain.

As in Garman and Klass (1980) and Ahelgebey et al. (2016b), we build the realized volatility as  $RV_t = 0.5 (\log H_t - \log L_t)^2 - (2 \log 2 - 1) (\log C_t - \log C_{t-1})^2$ , where  $H_t$ ,  $L_t$  and  $C_t$  denote the high, low and closing price of a given stock on day  $t$ , respectively and consider a VAR(1) model.

There is a strong evidence of sparsity with a probability of 0.16 of edge existence (Figure 4). Based on the posterior number of clusters, we identify five levels of linkage strengths, customarily called "negative" (blue), "weak positive" (green), "positive" (orange) and "strong positive" (red). Negative linkages imply some institutions react with a volatility decrease to positive volatility shocks, thus reducing systemic risk. Top plot in Figure 4 shows the coloured realized-volatility network. The node size increases with the node eigenvector centrality, which is evaluated on the overall network without accounting for the linkage strength. We find that insurance companies and banks (e.g., AGEAS and Bank of Ireland) are central and they present different type of linkages (e.g., see AGEAS two step ego network in middle plot). Also, a community or block structure can be detected with some small communities of same countries banks, such as the one related to the Italian (Monte dei Paschi and other Popular Banks) and Greek (Alpha Bank, National Bank of Greece, Bank of Piraeus) banks.

Evaluating the node eigenvector centrality on the subgraph of positive and strong positive linkages, we found that also real estates sector is central (e.g. Immofiz in the bottom plot). Our approach thus helps in better understanding the role of financial institutions in the buildup of the systemic risk, revealing different aspects of their activity and in particular for insurance and real estate industries.

## 5 Conclusions

This paper introduces a novel Bayesian nonparametric prior for VAR models, which allows both for shrinking coefficients toward multiple locations and for identifying groups of coefficients. In particular, we propose a two-stage hierarchical prior distribution, which combines Dirichlet process and Bayesian Lasso priors. The sparsity and the random partition induced by our hierarchical prior make our model particularly well suited for extracting networks which accounts for features observed in financial and economic networks such blocks, community structures, linkage strength heterogeneity.

The simulation studies illustrate the effectiveness of the MCMC algorithm and the good performance of our model in high dimension settings, compared to some existing priors, such as the Stochastic Search Variable Selection, Elastic-net and simple Bayesian Lasso.

In the macroeconomic application, we investigate the business shock transmission between different countries. Our new multiple shrinkage prior allows us to extract networks at different lags, to identify of the most relevant linkages among countries and to cluster linkages into groups. These results give us the opportunity to find evidence of three types of shock transmission effects: 'negative', 'positive' and 'strong positive'. We find that at certain lag, core European countries appear to be the countries that receive more shocks from other countries, while the periphery European countries transmit the highest percentage of shocks. Moreover, some countries which are not central in the global network, become central when only negative (or only positive) linkages are considered.

In the financial application, we find that a node can play different roles in the network topology reacting in various ways to volatility shocks from other nodes. Our methodology helps also in understanding the role of financial, insurance and real estate institutions in the economic system and their role in the build-up of systemic risk.

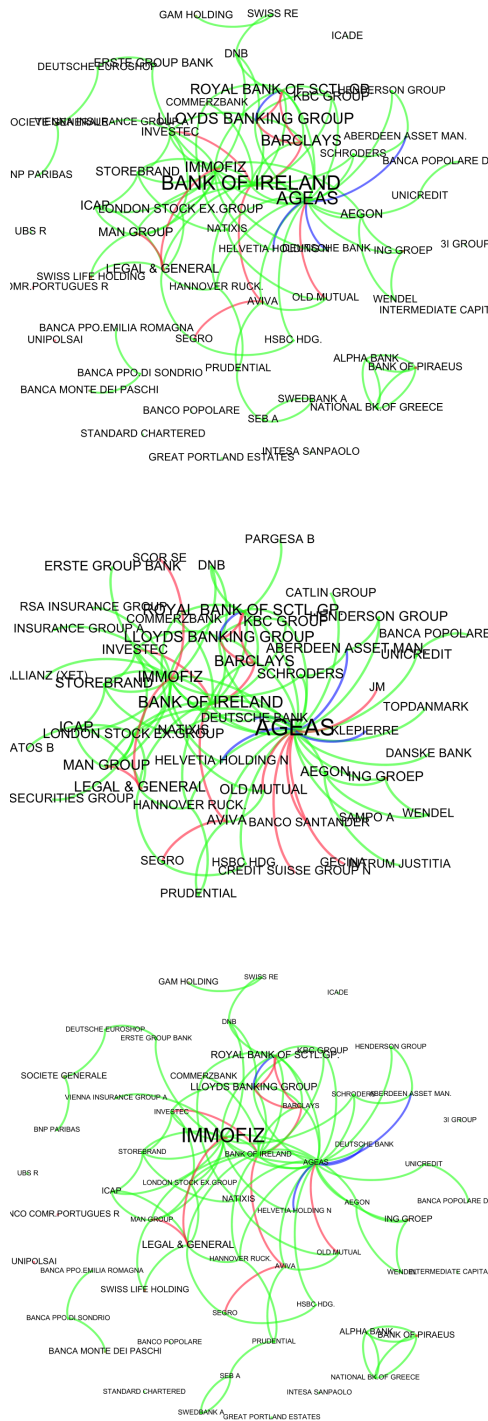


Figure 4: Weighted financial networks of Realized Volatility for different financial institutions of Euro Stoxx 600. Nodes' size is based on the node degree and the edges are clockwise-oriented.

## References

- Abramowitz, M. and Stegun, I. A. (1972). *Handbook of Mathematical Functions with Formulas, Graphs, and Mathematical Tables*. Dover, New York.
- Acharya, V. V., Engle, R., and Richardson, M. (2012). Capital Shortfall: A New Approach to Ranking and Regulating Systemic Risks. *American Economic Review*, 102(3):59–64.
- Ahelgebey, D. F., Billio, M., and Casarin, R. (2016a). Bayesian Graphical Models for Structural Vector Autoregressive Processes. *Journal of Applied Econometrics*, 31(2):357–386.
- Ahelgebey, D. F., Billio, M., and Casarin, R. (2016b). Sparse Graphical Vector Autoregression: A Bayesian Approach. *Annals of Economics and Statistics*, 123:333–361.
- Andrews, D. and Mallows, C. (1974). Scale mixtures of normal distributions. *Journal of the Royal Statistical Society Series B*, 36(1):99–102.
- Antoniak, C. (1974). Mixtures of dirichlet processes with applications to bayesian nonparametric problems. *Annals of Statistics*, 2:1152–1174.
- Barigozzi, M. and Brownlees, C. (2016). NETS: Network Estimation for Time Series. *Working Paper*.
- Bassetti, F., Casarin, R., and Leisen, F. (2014). Beta-product dependent Pitman-Yor processes for Bayesian inference. *Journal of Econometrics*, 180(1):49–72.
- Bianchi, D., Billio, M., Casarin, R., and Guidolin, M. (2018). Modeling systemic risk with Markov switching graphical SUR models. *Journal of Econometrics*, Forth.
- Billio, M., Casarin, R., Ravazzolo, F., and Van Dijk, H. (2016). Interactions between eurozone and US booms and busts: A Bayesian panel Markov-switching VAR model. *Journal of Applied Econometrics*, 31(7):1352–1370.
- Billio, M., Getmansky, M., Lo, A. W., and Pelizzon, L. (2012). Econometric measures of connectedness and systemic risk in the finance and insurance sectors. *Journal of Financial Econometrics*, 104(3):535–559.
- Canova, F. and Ciccarelli, M. (2004). Forecasting and turning point prediction in a Bayesian panel VAR model. *Journal of Econometrics*, 120(2):327–359.

- Carriero, A., Clark, T., and Marcellino, M. (2015). Bayesian VARs: Specification choices and forecast accuracy. *Journal of Applied Econometrics*, 30(1):46–73.
- Carvalho, C. M., Massam, H., and West, M. (2007). Simulation of hyper-inverse wishart distributions in graphical models. *Biometrika*, 94(3):647–659.
- Casarin, R., Costola, M., and Yenerdag, E. (2018). Financial bridges and network communities. Working paper.
- Chib, S. and Greenberg, E. (1995). Hierarchical analysis of SUR models with extensions to correlated serial errors and time-varying parameter models. *Journal of Econometrics*, 68(2):339–360.
- Dahl, D. B. (2006). Model-based clustering for expression data via a Dirichlet process mixture model. In Do, K.-A., Müller, P. P., and Vannucci, M., editors, *Bayesian Inference for Gene Expression and Proteomics*, pages 201–218. Cambridge University Press.
- Demirer, M., Diebold, F. X., Liu, L., and Yilmaz, K. (2018). Estimating Global Bank Network Connectedness. *Journal of Applied Econometrics*, 33(1):1–15.
- Di Lucca, M., Guglielmi, A., Muller, P., and Quintana, F. (2013). A simple class of bayesian nonparametric autoregression models. *Bayesian Anal.*, 8(1):63–88.
- Diebold, F. X. and Yilmaz, K. (2014). On the network topology of variance decompositions: Measuring the connectedness of financial firms. *Journal of Econometrics*, 182(1):119–134.
- Diebold, F. X. and Yilmaz, K. (2015). *Measuring the Dynamics of Global Business Cycle Connectedness*, pages 45–89. Oxford University Press.
- Diebold, F. X. and Yilmaz, K. (2016). Trans-Atlantic Equity Volatility Connectedness: U.S. and European Financial Institutions, 2004–2014. *Journal of Financial Econometrics*, 14(1):81–127.
- Doan, T., Litterman, R., and Sims, C. A. (1984). Forecasting and conditional projection using realistic prior distributions. *Econometric Reviews*, 3(1):1–100.
- Ferguson, T. S. (1973). A Bayesian Analysis of some Nonparametric Problems. *The Annals of Statistics*, 1(2):209–230.
- Francis, N., Owyang, M., and Savascin, O. (2017). An endogenously clustered factor approach to international business cycles. *Journal of Applied Econometrics*, 32(7):1261–1276.

- Garman, M. and Klass, M. (1980). On the estimation of security price volatilities from historical data. *Journal of Business*, 53:67–78.
- Gefang, D. (2014). Bayesian doubly adaptive elastic-net lasso for var shrinkage. *International Journal of Forecasting*, 30(1):1–11.
- George, E. I., Sun, D., and Ni, S. (2008). Bayesian stochastic search for VAR model restrictions. *Journal of Econometrics*, 142(1):553–580.
- Geweke, J. and Amisano, G. (2010). Comparing and evaluating Bayesian predictive distributions of asset returns. *International Journal of Forecasting*, 26(2):216–230.
- Giudici, P. and Green, P. (1999). Decomposable graphical Gaussian model determination. *Biometrika*, 86(4):758–801.
- Griffin, J. and Kalli, M. (2018). Bayesian nonparametric vector autoregressive models. *Journal of Econometrics*, 203(2):267–282.
- Griffin, J. and Steel, M. F. J. (2006a). Inference with non-gaussian ornstein–uhlenbeck processes for stochastic volatility. *Journal of Econometrics*, 134(2):605–644.
- Griffin, J. E. and Steel, M. F. J. (2006b). Order-based dependent Dirichlet processes. *Journal of the American Statistical Association*, 101(473):179–194.
- Griffin, J. E. and Steel, M. F. J. (2011). Stick-breaking autoregressive processes. *Journal of Econometrics*, 162(2):383–396.
- Hatjispyros, S. J., Nicolieris, T. N., and Walker, S. G. (2011). Dependent mixtures of Dirichlet processes. *Computational Statistics & Data Analysis*, 55(6):2011–2025.
- Hautsch, N., Schaumburg, J., and Schienle, M. (2015). Financial network systemic risk contributions. *Review of Finance*, 19:685–738.
- Hirano, K. (2002). Semiparametric Bayesian inference in autoregressive panel data models. *Econometrica*, 70(2):781–799.
- Hjort, N. L., Homes, C., Müller, P., and Walker, S. G. (2010). *Bayesian Nonparametrics*. Cambridge University Press.
- Jensen, J. M. and Maheu, M. J. (2010). Bayesian semiparametric stochastic volatility modeling. *Journal of Econometrics*, 157(2):306–316.



- Jones, B., Carvalho, C., Dobra, A., Hans, C., Carter, C., and West, M. (2005). Experiments in stochastic computation for high-dimensional graphical models. *Statistical Science*, 20(4):388–400.
- Kalli, M., Griffin, J. E., and Walker, S. G. (2011). Slice sampling mixture models. *Statistics and Computing*, 21(1):93–105.
- Kaufmann, S. (2010). Dating and forecasting turning points by Bayesian clustering with dynamic structure: a suggestion with an application to Austrian data. *Journal of Applied Econometrics*, 25(2):309–344.
- Kaufmann, S. and Schumacher, C. (2017). Identifying relevant and irrelevant variables in sparse factor models. *Journal of Applied Econometrics*, 32(6):1123–1144.
- Kolossiatos, M., Griffin, J., and Steel, M. F. J. (2013). On Bayesian nonparametric modelling of two correlated distributions. *Statistics and Computing*, 23:1–15.
- Koop, G. (2013). Forecasting with medium and large Bayesian VARs. *Journal of Applied Econometrics*, 28(2):177–203.
- Koop, G. and Korobilis, D. (2010). Bayesian multivariate time series methods for empirical macroeconomics. *Foundations and Trends in Econometrics*, 3(4):267–358.
- Koop, G. and Korobilis, D. (2016). Model uncertainty in panel vector autoregressions. *European Economic Review*, 81:115–131.
- Korobilis, D. (2013). VAR forecasting using Bayesian variable selection. *Journal of Applied Econometrics*, 28(2):204–230.
- Korobilis, D. (2016). Prior selection for panel vector autoregressions. *Computational Statistics & Data Analysis*, 101:110–120.
- Kose, M. A., Otrok, C., and Whiteman, C. H. (2003). International Business Cycles: World, region and country specific factors. *American Economic Review*, 93(4):1216–1239.
- Kose, M. A., Otrok, C., and Whiteman, C. H. (2010). Understanding the evolution of world business cycles. *Journal of International Economics*, 75(1):110–130.
- Litterman, R. (1986). Forecasting with Bayesian vector autoregressions-five years of experience. *Journal of Business and Economic Statistics*, 4(1):25–38.

- Lo, A. Y. (1984). On a class of Bayesian nonparametric estimates: I. density estimates. *The Annals of Statistics*, 12(1):351–357.
- MacEachern, S. N. (1999). Dependent nonparametric processes. In *In ASA Proceedings of the Section on Bayesian Statistical Science, Alexandria, VA*, pages 50–55. American Statistical Association.
- MacEachern, S. N. (2001). Decision theoretic aspects of dependent nonparametric processes. In George, E., editor, *Bayesian Methods with Applications to Science, Policy and Official Statistics*, pages 551–560. Creta: ISBA.
- MacLehose, R. and Dunson, D. (2010). Bayesian semiparametric multiple shrinkage. *Biometrics*, 66(2):455–462.
- Magnus, J. R. and Neudecker, H. (1999). *Matrix Differential Calculus with Applications in Statistics and Econometrics, 2nd Edition*. John Wiley.
- Miller, R. (1980). Bayesian analysis of the two-parameter gamma distribution. *Technometrics*, 22(1):65–69.
- Min, C. and Zellner, A. (1993). Bayesian and non-Bayesian methods for combining models and forecasts with applications to forecasting international growth rates. *Journal of Econometrics*, 56(1-2):89–118.
- Müller, P., Quintana, F., and Rosner, G. (2004). A method for combining inference across related nonparametric Bayesian models. *Journal of the Royal Statistical Society B*, 66:735–749.
- NietoBarajas, L. E. and Quintana, F. A. (2016). A bayesian nonparametric dynamic ar model for multiple time series analysis. *Journal of Time Series Analysis*, 37(5):675–689.
- Park, T. and Casella, G. (2008). The Bayesian Lasso. *Journal of the American Statistical Association*, 103(482):681–686.
- Pennell, M. L. and Dunson, D. B. (2006). Bayesian semiparametric dynamic frailty models for multiple event time data. *Biometrics*, 62:1044–1052.
- Richardson, S. and Green, P. J. (1997). On bayesian analysis of mixtures with an unknown number of components. *Journal of the Royal Statistical Society Series B*, 59:731–792.
- Rodriguez, A. and ter Horst, E. (2008). Bayesian dynamics density estimation. *Bayesian Analysis*, 3(2):339–365.

- Scott, S. L. and Varian, H. R. (2014). Predicting the present with Bayesian structural time series. *International Journal of Mathematical Modelling and Numerical Optimisation*, 5(1-2):4–23.
- Sethuraman, J. (1994). A constructive definition of the Dirichlet process prior. *Statistica Sinica*, 4:639–650.
- Sims, C. A. (1980). Macroeconomics and reality. *Econometrica*, 48(1):1–48.
- Sims, C. A. (1992). Interpreting the macroeconomic time series facts: The effects of monetary policy. *European Economic Review*, 36(5):975–1000.
- Sims, C. A. and Zha, T. (1998). Bayesian methods for dynamic multivariate models. *International Economic Review*, 39(4):949–968.
- Stock, J. H. and Watson, M. W. (2012). Generalized shrinkage methods for forecasting using many predictors. *Journal of Business & Economic Statistics*, 30(4):481–493.
- Taddy, M. A. (2010). An auto-regressive mixture model for dynamic spatial Poisson processes: Application to tracking the intensity of violent crime. *Journal of the American Statistical Association*, 105(492):1403–1417.
- Taddy, M. A. and Kottas, A. (2009). Markov switching Dirichlet process mixture regression. *Bayesian Analysis*, 4(4):793–816.
- Teh, Y. (2011). Dirichlet process. In *Encyclopedia of Machine Learning*, pages 280–287. Springer.
- Tibshirani, R. (1996). Regression shrinkage and selection via the lasso. *Journal of the Royal Statistical Society Series B*, 58(1):267–288.
- Walker, S. G. (2007). Sampling the Dirichlet mixture model with slices. *Communications in Statistics - Simulation and Computation*, 36(1):45–54.
- Wang, H. (2010). Sparse seemingly unrelated regression modelling: Applications in finance and econometrics. *Computational Statistics & Data Analysis*, 54(11):2866–2877.
- Zou, H. and Hastie, T. (2005). Regularization and variable selection via the elastic net. *Journal of the Royal Statistical Society B*, 67(2):301–320.
- Zou, H. and Zhang, H. H. (2009). On the adaptive elastic-net with diverging number of parameters. *Annals of Statistics*, 37(4):1733–1751.

## A Further details on prior specification

### A.1 Normal-Gamma distribution

A normal-gamma random variable  $X \sim \mathcal{NG}(\mu, \gamma, \tau)$  has probability density function

$$f(x|\mu, \gamma, \tau) = \frac{\tau^{\frac{2\gamma+1}{4}} |x - \mu|^{\gamma - \frac{1}{2}}}{2^{\gamma - \frac{1}{2}} \sqrt{\pi} \Gamma(\gamma)} K_{\gamma - \frac{1}{2}}(\sqrt{\tau} |x - \mu|),$$

where  $K_\gamma(\cdot)$  represents the modified Bessel function of the second kind with index  $\gamma$  (see Abramowitz and Stegun (1972)),  $\mu \in \mathbb{R}$  is the location parameter,  $\gamma > 0$  is the shape parameter and  $\tau > 0$  is the scale parameter. The normal-gamma distribution has the double exponential distribution as a special case for  $\gamma = 1$  and can be represented as a scale mixture of normals (Andrews and Mallows (1974)),

$$\mathcal{NG}(x|\mu, \gamma, \tau) = \int_0^{+\infty} \mathcal{N}(x|\mu, \lambda) \mathcal{Ga}(\lambda|\gamma, \tau/2) d\lambda, \quad (\text{A.1})$$

where  $\mathcal{Ga}(\cdot|a, b)$  denotes a gamma distribution with mean  $a/b$  and variance  $a/b^2$ .

### A.2 Gamma scale-shape distribution

A Gamma scale-shape random vector  $(X, Y) \sim \mathcal{GS}(\nu, p, s, n)$  has pdf

$$g(x, y|\nu, p, s, n) \propto \tau^{\nu x - 1} p^{x-1} \exp\{-sy\} \frac{1}{\Gamma(x)^n}, \quad (\text{A.2})$$

with parameters  $\nu > 0$ ,  $p > 0$ ,  $s > 0$  and  $n > 0$  (see Miller (1980)). The pdf in equation (A.2) factorizes as  $g(x, y) = g(y|x)g(x)$ , where

$$g(y|x) = \frac{g(x, y)}{g(x)} = \frac{\tau^{\nu x - 1} e^{-sy}}{\Gamma(\nu x)} s^{\nu x}$$

that is a density of a  $\mathcal{Ga}(\nu x, s)$ , and

$$g(x) = \int_0^\infty g(x, y) dy = C \frac{\Gamma(\nu x) p^{x-1}}{\Gamma(x)^n s^{\nu x}}$$

is the marginal density with normalizing constant  $C$  such that  $\int_0^\infty g(x) dx = 1$ . We show in Figure A.1 the density function,  $g(x)$ , for the two parameter settings used in the empirical application:  $\nu = 30$ ,  $s = 1/30$ ,  $p = 0.5$  and  $n = 18$  (dashed line) and  $\nu = 3$ ,  $s = 1/3$ ,  $p = 0.5$  and  $n = 10$  (solid line).

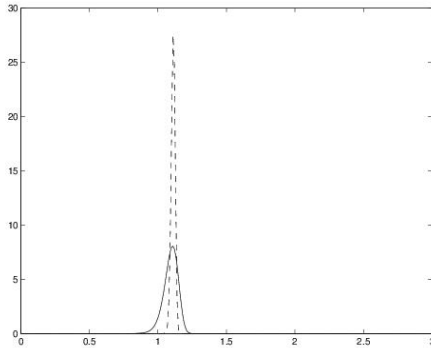


Figure A.1: Probability density function,  $g(x)$ , for sparse (dashed line) and non-sparse (solid line) case, respectively.

### A.3 Hyper-inverse Wishart Distribution

An Hyper-inverse Wishart random variable  $\Sigma \sim \mathcal{HIW}_G(b, L)$  has pdf

$$p(\Sigma) = \prod_{P \in \mathcal{P}} p(\Sigma_P) \left( \prod_{S \in \mathcal{S}} p(\Sigma_S) \right)^{-1},$$

where  $\mathcal{S} = \{S_1, \dots, S_{n_S}\}$  and  $\mathcal{P} = \{P_1, \dots, P_{n_P}\}$  are the set of separators and of prime components, respectively, of the graph  $G$ . In particular,  $b$  is the degree of freedom,  $L$  is the scale matrix and

$$p(\Sigma_P) \propto |\Sigma_P|^{-(b+2\text{Card}(P))/2} \exp \left\{ -\frac{1}{2} \text{tr}(\Sigma_P^{-1} L_P) \right\},$$

with  $L_P$  the positive-definite symmetric diagonal block of  $L$  corresponding to  $\Sigma_P$ .

### A.4 Dirichlet Process prior

The Dirichlet Process,  $\text{DP}(\tilde{\alpha}, H)$ , can be defined by using the stick-breaking representation (Sethuraman (1994)) given by:

$$\mathbb{P}_i(\cdot) = \sum_{j=1}^{\infty} w_{ij} \delta_{\{\theta_{ij}\}}(\cdot), \quad i = 1, \dots, M.$$

Following the definition of the dependent stick-breaking processes (see MacEachern (1999) and MacEachern (2001)), the atoms  $\theta_{ij}$  are i.i.d. sequences of random

elements with probability distribution  $H$  ( $\theta_{ij} \stackrel{\text{i.i.d.}}{\sim} H$ ); and the weights  $w_{ij}$  are determined through the stick-breaking construction, for  $j = 1$ ,  $w_{i1} = v_{i1}$  and for  $j > 1$

$$w_{ij} = v_{ij} \prod_{k=1}^{j-1} (1 - v_{ik}), \quad i = 1, \dots, M$$

with  $v_j = (v_{1j}, \dots, v_{Mj})$  independent random variables taking values in  $[0, 1]^M$  distributed as a  $\mathcal{B}e(1, \tilde{\alpha})$  such that  $\sum_{j \geq 1} w_{ij} = 1$  almost surely for every  $i$ .

## B Proof of the results in the paper

*Proof of result in Eq. (11).* Let  $K(\boldsymbol{\beta}_i | \boldsymbol{\theta}_i)$  be the joint density kernel of the sequence  $\beta_{ij} \stackrel{\text{i.i.d.}}{\sim} \mathcal{NG}(\beta_{ij} | \boldsymbol{\theta}_{ij}^*)$ ,  $j = 1, \dots, n_i$  and  $\boldsymbol{\theta}_{ij}^* | \mathbb{Q}_i \stackrel{\text{i.i.d.}}{\sim} \mathbb{Q}_i$ , the atoms of the random probability measure  $\mathbb{Q}_i$ . Let  $f_i(\boldsymbol{\beta}_i | \mathbb{Q}_i)$  be the random probability density function obtained by integrating out the random measure  $\mathbb{Q}_i$  (Lo (1984)):

$$f_i(\boldsymbol{\beta}_i | \mathbb{Q}_i) = \int K(\boldsymbol{\beta}_i | \boldsymbol{\theta}_i) \mathbb{Q}_i(d\boldsymbol{\theta}_i). \quad (\text{B.1})$$

Using the definition of  $\mathbb{Q}_i$  as a convex combination of a sparse component and a DPP in equation (6), we obtain

$$f_i(\boldsymbol{\beta}_i | \mathbb{Q}_i) = \pi_i \int K(\boldsymbol{\beta}_i | \boldsymbol{\theta}_i) \mathbb{P}_0(d\boldsymbol{\theta}_i) + (1 - \pi_i) \int K(\boldsymbol{\beta}_i | \boldsymbol{\theta}_i) \mathbb{P}_i(d\boldsymbol{\theta}_i) \quad (\text{B.2})$$

We use the stick-breaking representation of the DPP (Appendix A) and get

$$\begin{aligned} f_i(\boldsymbol{\beta}_i | \mathbb{Q}_i) &= \pi_i \int \mathcal{NG}(\boldsymbol{\beta}_i | \boldsymbol{\mu}, \boldsymbol{\gamma}, \boldsymbol{\tau}) \mathbb{P}_0(d(\boldsymbol{\mu}, \boldsymbol{\gamma}, \boldsymbol{\tau})) + (1 - \pi_i) \int \mathcal{NG}(\boldsymbol{\beta}_i | \boldsymbol{\mu}, \boldsymbol{\gamma}, \boldsymbol{\tau}) \mathbb{P}_i(d(\boldsymbol{\mu}, \boldsymbol{\gamma}, \boldsymbol{\tau})) \\ &= \pi_i \mathcal{NG}(\boldsymbol{\beta}_i | 0, \gamma_0, \tau_0) + (1 - \pi_i) \sum_{k=1}^{\infty} w_{ik} \mathcal{NG}(\boldsymbol{\beta}_i | \mu_{ik}, \gamma_{ik}, \tau_{ik}) \end{aligned} \quad (\text{B.3})$$

By defining,

$$\check{w}_{ik} = \begin{cases} \pi_i, & k = 0, \\ (1 - \pi_i)w_{ik}, & k > 0, \end{cases} \quad \check{\theta}_{ik} = \begin{cases} (0, \gamma_0, \tau_0), & k = 0, \\ (\mu_{ik}, \gamma_{ik}, \tau_{ik}), & k > 0. \end{cases}$$

we have the infinite mixture representation

$$f_i(\boldsymbol{\beta}_i | \mathbb{Q}_i) = \sum_{k=0}^{\infty} \check{w}_{ik} \mathcal{NG}(\boldsymbol{\beta}_i | \check{\theta}_{ik}).$$

□

*Proof of result in Eq. (13).* We introduce a set of slice latent variables,  $u_{ij}, j = 1, \dots, n_i$ , which allows us to represent the full conditional of  $\beta_{ij}$  as follows,

$$\begin{aligned} f_i(\beta_{ij}, u_{ij} | (\mu_i, \gamma_i, \tau_i), w_i) &= \pi_i \sum_{k=0}^{\infty} \mathbb{I}(u_{ij} < \tilde{w}_{ik}) \mathcal{NG}(\beta_{ij} | (0, \gamma_{ik}, \tau_{ik})) + \\ &+ (1 - \pi_i) \sum_{k=1}^{\infty} \mathbb{I}(u_{ij} < w_{ik}) \mathcal{NG}(\beta_{ij} | \mu_{ik}, \gamma_{ik}, \tau_{ik}) \\ &= \pi_i \mathbb{I}(u_{ij} < \tilde{w}_0) \mathcal{NG}(\beta_{ij} | (0, \gamma_0, \tau_0)) + (1 - \pi_i) \sum_{k=1}^{\infty} \mathbb{I}(u_{ij} < w_{ik}) \mathcal{NG}(\beta_{ij} | \mu_{ik}, \gamma_{ik}, \tau_{ik}), \end{aligned}$$

where  $\tilde{w}_{ik} = \tilde{w}_0 = 1$  if  $k = 0$  and  $\tilde{w}_{ik} = 0$  for  $k > 0$  and, for simplicity of notations, we denote  $(0, \gamma_{i0}, \tau_{i0}) = (0, \gamma_0, \tau_0)$ .

The slice variables allow us to represent the infinite mixture as a finite mixture conditionally on a random number of components. More specifically, define the set

$$\mathcal{A}_{w_i}(u_{ij}) = \{k : u_{ij} < w_{ik}\}, \quad j = 1, \dots, n_i,$$

then it can be proved that the cardinality of  $\mathcal{A}_{w_i}$  is almost surely finite. Posterior draws for  $u_{ij}$  are easily obtained by slice sampling.

The conditional joint pdf for  $\beta_{ij}$  and  $u_{ij}$ ,  $f_i(\beta_{ij}, u_{ij} | (\mu_i, \gamma_i, \tau_i), w_i)$ , is equal to

$$\pi_i \mathbb{I}(u_{ij} < \tilde{w}_0) \mathcal{NG}(\beta_{ij} | 0, \gamma_0, \tau_0) + (1 - \pi_i) \sum_{k \in \mathcal{A}_{w_i}(u_{ij})} \mathcal{NG}(\beta_{ij} | \mu_{ik}, \gamma_{ik}, \tau_{ik}).$$

We iterate the data augmentation principle and for each  $f_i$  we introduce two allocation variables  $\xi_{ij}$  and  $d_{ij}$ , associated with the sparse and non-sparse components, respectively, of the random measure  $\mathbb{Q}_i$ . The joint pdf is

$$\begin{aligned} f_i(\beta_{ij}, u_{ij}, d_{ij}, \xi_{ij}) &= (\pi_i \mathbb{I}(u_{ij} < \tilde{w}_{d_{ij}}) \mathcal{NG}(\beta_{ij} | 0, \gamma_0, \tau_0))^{1-\xi_{ij}} \cdot \\ &((1 - \pi_i) \mathbb{I}(u_{ij} < w_{id_{ij}}) \mathcal{NG}(\beta_{ij} | \mu_{id_{ij}}, \gamma_{id_{ij}}, \tau_{id_{ij}}))^{\xi_{ij}}. \end{aligned}$$

From (4), we de-marginalize the Normal-Gamma distribution by introducing a latent variable  $\lambda_{ij}$  for each  $\beta_{ij}$  and conclude that the joint distribution is

$$\begin{aligned} f_i(\beta_{ij}, \lambda_{ij}, u_{ij}, d_{ij}, \xi_{ij}) &= (\mathbb{I}(u_{ij} < \tilde{w}_{d_{ij}}) \mathcal{N}(\beta_{ij} | 0, \lambda_{ij}) \mathcal{Ga}(\lambda_{ij} | \gamma_0, \tau_0/2))^{1-\xi_{ij}} \cdot \\ &(\mathbb{I}(u_{ij} < w_{id_{ij}}) \mathcal{N}(\beta_{ij} | \mu_{id_{ij}}, \lambda_{ij}) \mathcal{Ga}(\lambda_{ij} | \gamma_{id_{ij}}, \tau_{id_{ij}}/2))^{\xi_{ij}} \pi_i^{1-\xi_{ij}} (1 - \pi_i)^{\xi_{ij}}. \end{aligned}$$

□

## C Gibbs sampling details

We introduce for  $k \geq 1$  the set of indexes of the coefficients allocated to the  $k$ -th mixture component,  $\mathcal{D}_{ik} = \{j \in 1, \dots, n_i : d_{ij} = k, \xi_{ij} = 1\}$  and the set of the non-empty mixture components,  $\mathcal{D}^* = \{k | \cup_i \mathcal{D}_{ik} \neq \emptyset\}$ . The number of stick-breaking components is denoted by  $D^* = \max_i \{\max_{j \in \{1, \dots, n_i\}} d_{ij}\}$ . As noted by Kalli et al. (2011), the sampling of infinitely many elements of  $\Theta$  and  $V$  is not necessarily, since only the elements in the full conditional distributions of  $(D, \Xi)$  are needed and the maximum number is  $N^* = \max_i \{N_i^*\}$ , where  $N_i^*$  is the smallest integer such that  $\sum_{k=1}^{N_i^*} w_{ik} > 1 - u_i^*$ , where  $u_i^* = \min_{1 \leq j \leq n_i} \{u_{ij}\}$ .

### Update the stick-breaking and slice variables $V$ and $U$

We treat  $V$  as three blocks:  $V^* = \{V_k : k \in \mathcal{D}^*\}$ ,  $V^{**} = (v_{kD^*+1}, \dots, v_{kN^*})$  and  $V^{***} = \{V_k : k > N^*\}$ . In order to sample  $(U, V)$ , a further blocking is used:

- i) Sampling from the full conditional of  $V^*$ , by using

$$f(v_{ij} | \dots) \propto \mathcal{B}e \left( 1 + \sum_{j=1}^{n_i} \mathbb{I}(d_{ij} = d, \xi_{ij} = 1), \alpha + \sum_{j=1}^{n_i} \mathbb{I}(d_{ij} > d, \xi_{ij} = 1) \right).$$

for  $k \leq D^*$ . The elements of  $(V^{**}, V^{***})$  are sampled from the prior  $\mathcal{B}e(1, \alpha)$ .

- ii) Sampling from full conditional posterior distribution of  $U$

$$f(u_{ij} | \dots) \propto \begin{cases} \mathbb{I}(u_{ij} < w_{1d_{ij}})^{\xi_{ij}} & \text{if } \xi_{ij} = 1, \\ \mathbb{I}(u_{ij} < 1)^{1-\xi_{ij}} & \text{if } \xi_{ij} = 0, \end{cases}$$

### Update the mixing parameters $\lambda$

Regarding the mixing parameters  $\lambda_{ij}$ , the full conditional posterior distribution is

$$f(\lambda_{ij} | \dots) \propto \lambda_{ij}^{C_{ij}-1} \exp \left\{ -\frac{1}{2} \left[ A_{ij} \lambda_{ij} + \frac{B_{ij}}{\lambda_{ij}} \right] \right\} \propto \mathcal{G}i\mathcal{G}(A_{ij}, B_{ij}, C_{ij}),$$

where  $\mathcal{G}i\mathcal{G}$  denotes a Generalize Inverse Gaussian with  $A_{ij} > 0$ ,  $B_{ij} > 0$  and  $C_{ij} \in \mathbb{R}$

$$A_{ij} = [(1 - \xi_{ij})\tau_0 + \xi_{ij}\tau_{id_{ij}}], \quad B_{ij} = [(1 - \xi_{ij})\beta_{ij}^2 + \xi_{ij}(\beta_{ij} - \mu_{id_{ij}})^2], \\ C_{ij} = \left[ (1 - \xi_{ij})\gamma_0 + \gamma_{id_{ij}}\xi_{ij} - \frac{1}{2} \right].$$

The matrix  $\Lambda_i = \text{diag}\{\boldsymbol{\lambda}_i\}$  has the elements of  $\boldsymbol{\lambda}_i = (\lambda_{i1}, \dots, \lambda_{in_i})'$  on the diagonal.



### Update the atoms $\Theta$

We consider the sparse and the non-sparse case. In the sparse case, the full conditional distribution of  $\mu_0$  is  $f(\mu_0|\dots) = \delta_{\{0\}}(\mu_0)$  and the full conditional distribution of  $(\gamma_0, \tau_0)$  is:

$$f((\gamma_0, \tau_0)|\dots) \propto \mathcal{GS} \left( \gamma_0, \tau_0 | \nu_0 + \sum_{i=1}^M n_{i,0}, p_0 \prod_{i=1}^M \prod_{j|\xi_{ij}=0} \lambda_{ij}, s_0 + \frac{1}{2} \sum_{i=1}^M \sum_{j|\xi_{ij}=0} \lambda_{ij}, n_0 + \sum_{i=1}^M n_{i,0} \right),$$

where we assume  $n_{i,0} = \sum_{j=1}^{n_i} (1 - \xi_{ij}) = n_i - n_{i,1}$  and  $n_{i,1} = \sum_{j=1}^{n_i} \xi_{ij}$ . In the non-sparse case, we generate samples  $(\mu_{ik}, \gamma_{ik}, \tau_{ik})$ ,  $k = 1, \dots, N^*$ , by applying a single move Gibbs sampler. The full conditional for  $\mu_{ik}$  is

$$f(\mu_{ik}|\dots) \propto \mathcal{N}(\mu_{ik}|c, d) \prod_{j|\xi_{ij}=1, d_{ij}=k} \mathcal{N}(\beta_{ij}|\mu_{ik}, \lambda_{ij}) \propto \mathcal{N}(\tilde{E}_k, \tilde{V}_k)$$

with  $\tilde{E}_k = \tilde{V}_k \left( \frac{c}{d} + \sum_{j|\xi_{ij}=1, d_{ij}=k} \frac{\beta_{ij}}{\lambda_{ij}} \right)$  and  $\tilde{V}_k = \left( \frac{1}{d} + \sum_{j|\xi_{ij}=1, d_{ij}=k} \frac{1}{\lambda_{ij}} \right)^{-1}$ , the mean and variance, respectively. The joint conditional posterior of  $(\gamma_{ik}, \tau_{ik})$  is:

$$f((\gamma_{ik}, \tau_{ik})|\dots) \propto \mathcal{GS} \left( \gamma_{ik}, \tau_{ik} | \nu_1 + n_{i,1k}, p_1 \prod_{j|\xi_{ij}=1, d_{ij}=k} \lambda_{ij}, s_1 + \frac{1}{2} \sum_{j|\xi_{ij}=1, d_{ij}=k} \lambda_{ij}, n_1 + n_{i,1k} \right),$$

for  $k \in \mathcal{D}^*$ , where  $n_{i,1k} = \sum_{j=1}^{n_i} \xi_{ij} \mathbb{1}(d_{ij} = k)$  and from the prior  $H$  for  $k \notin \mathcal{D}^*$ . In order to draw samples from  $\mathcal{GS}$  in both cases, we apply a collapsed Gibbs sampler. Samples from  $f(\gamma)$  are obtained by a Metropolis-Hastings (MH) algorithm and samples from  $f(\tau|\gamma)$  are obtained from a Gamma distribution.

### Update the coefficients $\beta$

The full conditional posterior distribution of  $\beta$  is:

$$f(\beta_i|\dots) \propto \mathcal{N}_{n_i}(\tilde{\mathbf{v}}_i, M_i),$$

with mean  $\tilde{\mathbf{v}}_i = M_i (\sum_t X_t' \Sigma^{-1} \mathbf{y}_t + \Lambda_i^{-1} (\boldsymbol{\mu}_i^* \odot \boldsymbol{\xi}_i))$  and variance  $M_i = (\sum_t X_t' \Sigma^{-1} X_t + \Lambda_i^{-1})^{-1}$ ; and  $\boldsymbol{\mu}_i^* = (\mu_{id_{i1}}, \dots, \mu_{id_{i n_i}})'$ ,  $\boldsymbol{\xi}_i = (\xi_{i1}, \dots, \xi_{i n_i})'$ .

### Update the covariance matrix $\Sigma$

By using the sets  $\mathcal{S}$  and  $\mathcal{P}$  as described in Appendix A and a decomposable graph, the likelihood of the graphical Gaussian model can be approximated as the ratio

between the likelihood in the prime and in the separator components. Thus, the posterior for  $\Sigma$  factorizes as follows:

$$p(\Sigma|\dots) \propto \mathcal{HITW}_G \left( b + T, L + \sum_{t=1}^T (y_t - X'_t \boldsymbol{\beta})'(y_t - X'_t \boldsymbol{\beta}) \right).$$

### Update the graph $G$

We apply a MCMC for multivariate graphical models for  $G$  (see Giudici and Green (1999) and Jones et al. (2005)) and due to prior independence assumption,

$$p(\mathbf{y}|G) = \iint \prod_{t=1}^T (2\pi)^{-n/2} |\Sigma|^{-n/2} \exp \left( -\frac{1}{2} (y_t - X'_t \boldsymbol{\beta}) \Sigma^{-1} (y_t - X'_t \boldsymbol{\beta}) \right) p(\boldsymbol{\beta}) p(\Sigma|G) d\boldsymbol{\beta} d\Sigma.$$

Following Jones et al. (2005) we apply a local-move MH based on the conditional posterior  $p(G|\dots)$  with an add/delete edge move proposal.

### Update the allocation variables $D$ and $\Xi$

Sampling from the full conditional of  $D$  is obtained from

$$P(d_{ij} = d, \xi_{ij} = 1 | \dots) \propto \frac{(1 - \pi_i) \mathcal{N}(\beta_{ij} | \mu_{id}, \lambda_{ij}) \mathcal{G}a(\lambda_{ij} | \gamma_{id}, \tau_{id}/2)}{\sum_{k \in A_{w_i}(u_{ij})} \mathcal{N}(\beta_{ij} | \mu_{ik}, \lambda_{ij}) \mathcal{G}a(\lambda_{ij} | \gamma_{ik}, \tau_{ik}/2)}$$

in the non-sparse case for every  $d \in A_{w_i}(u_{ij})$ . While in the sparse case, from

$$P(d_{ij} = d, \xi_{ij} = 0 | \dots) \propto \pi_i \mathbb{I}(u_{ij} < \tilde{w}_{id}), \quad d \in A_{\tilde{w}}(u_{ij})$$

where  $A_{\tilde{w}}(u_{ij}) = \{k : u_{ij} < \tilde{w}_k\} = \{0\}$ , because  $\tilde{w}_k = 0, \forall k > 0$ ,

$$P(d_{ij} = d, \xi_{ij} = 0 | \dots) \propto \begin{cases} \pi_i \mathbb{I}(u_{ij} < 1) \mathcal{N}(\beta_{ij} | 0, \lambda_{ij}) \mathcal{G}a(\lambda_{ij} | \gamma_0, \tau_0/2) & \text{if } d = 0, \\ 0 & \text{if } d > 0. \end{cases}$$

### Update the prior restriction probabilities $\pi$

The full conditional for  $\pi_i$  is,

$$f(\pi_i | \dots) \propto \mathcal{B}e \left( n_i + 1 - \sum_{i=1}^{n_i} \mathbb{I}(\xi_{ii} = 1), \alpha_i + \sum_{i=1}^{n_i} \mathbb{I}(\xi_{ii} = 1) \right).$$